World Journal of Pharmaceutical Sciences
ISSN (Print): 2321-3310; ISSN (Online): 2321-3086
Published by Atom and Cell Publishers © All Rights Reserved
Available online at: http://www.wjpsonline.org/
Original Article

Phycosynthesis and photocatalytic degradation of methyl orange using silver nanoparticles synthesized by the *Sargassum wightii*

G. Ganapathy Selvam and K. Sivakumar

Division of Algal Biotechnology, Department of Botany, Annamalai University, Annamalainagar - 608 002, Tamil Nadu, India

Received: 21-07-2014 / Revised: 21-08-2014 / Accepted: 24-08-2014

ABSTRACTS

The present study was demonstrated with simple and rapid synthesis of silver (Ag) nanoparticles using marine seaweed, *Sargassum wightii*. The nanoparticles of silver were formed by the reduction of silver nitrate to aqueous silver metal ions during exposure to the extract of marine seaweed *S. wightii*. The optical properties of the obtained silver nanoparticles were characterized using UV–visible absorption and room temperature photoluminescence. The X-ray diffraction results reveal that the synthesized silver nanoparticles are in the cubic phase. The existence of functional groups was identified using Fourier transform infrared spectroscopy. The morphology and size of the synthesized particles were studied with atomic force microscope and Scanning electron microscope measurements. Further, the photocatalytic degradation of methyl orange was measured spectrophotometrically by using silver as nanocatalyst under visible light illumination. The results revealed that biosynthesized silver nanoparticles using *S. wightii* was found to be impressive in degrading methyl orange.

Keywords: Ag nanoparticles, *Sargassum wightii*, FT-IR, XRD, SEM, AFM

INTRODUCTION

The field of nanotechnology is one of the most active areas of research in modern materials science. Nanoparticles exhibit completely new or improved properties based on specific characteristics such as size, distribution and morphology. New applications of nanoparticles and nanomaterials are emerging rapidly (Jahn 1999; Naiwa 2000; Murphy 2008). Alexander the Great used silver vessels to store drinking water (Silver *et al*., 2006). However, the formulation of silver has changed during antiquity, from bulk silver to ionic silver or adsorbed on carrier materials (Zeolite) (Kwakye- Awwah *et al*., 2008) and now to silver nanoparticles.

The metallic nanoparticles are most promising and remarkable biomedical agents. Due to their large surface volume ratio, they govern interest of researchers on microbial resistance. Among the developed nanoparticles, silver (Ag) nanoparticles are pertaining to have a wide range of application in the fields of physical, chemical and biological science. In the past decade, several kinds of the biological organisms like microbes, plants and seaweeds have been employed and well studied for the synthesis of Ag nanoparticles (Ramanathan *et al*., 2011; Ahmad *et al*., 2003; Shankar *et al*., 2003; Mohanpuria *et al*., 2008; Kumar *et al*., 2012a). In the present study, the extracellular synthesis of silver nanoparticles by the brown seaweed *S. wightii* and their photocatalytic degradation of methyl orange using Ag nanoparticles synthesized from *S. wightii*.

MATERIALS AND METHODS

Plant material and preparation of the Extract: *Sargassum wightii* was used to make the aqueous extract. *Sargassum wightii* weighing 25g were thoroughly washed in distilled water, dried, cut into fine pieces and were crushed into 100 ml sterile distilled water and filtered through Whatman No.1 filter paper (pore size 25 µm). The filtrate was further filtered through 0.6 µm sized filters.

Synthesis of Silver Nanoparticles: 1mM aqueous solution of Silver nitrate ($AgNO_3$) was prepared and used for the synthesis of silver nanoparticles. 10 ml of *Sargassum wightii* extract was added into 90 ml of aqueous solution of 1 mM Silver nitrate

***Corresponding Author Address: Dr. K. Sivakumar,** Division of Algal Biotechnology, Department of Botany, Annamalai University, Annamalainagar - 608 002, Tamil Nadu, India; E-mail: kshivam69@gmail.com*

for reduction into Ag+ ions and kept at room temperature for 5 hours.

UV-Vis Spectra analysis: The reduction of pure Ag+ ions was monitored by measuring the UV-Vis spectrum of the reaction medium at 5 hours after diluting a small aliquot of the sample into distilled water. UV-Vis spectral analysis was done by using UV-Vis spectrophotometer UV-2450 (Shimadzu).

FTIR analysis of dried biomass after bioreduction: To remove any free biomass residue or compound that is not the capping ligand of the nanoparticles, the residual solution of 100 ml after reaction was centrifuged at 5000 rpm for 10 min and the resulting suspension was redispersed in 10 ml sterile distilled water. The centrifuging and redispersing process was repeated three times. Thereafter, the purified suspension was freeze dried to obtain dried powder. Finally, the dried nanoparticles were analysed by FTIR.

XRD measurement: The silver nanoparticle solution thus obtained was purified by repeated centrifugation at 5000 rpm for 20 min followed by redispersion of the pellet of silver nanoparticles into 10 ml of deionized water. After freeze drying of the purified silver particles, the structure and composition were analysed by XRD and SEM. The dried mixture of silver nanoparticles was collected for the determination of the formation of Ag nanoparticles by an X'Pert Pro x-ray diffractometer operated at a voltage of 40 kV and a current of 30 mA with Cu Kα radiation in θ- 2 θ configurations. The crystallite domain size was calculated from the width of the XRD peaks, assuming that they are free from non-uniform strains, using the Scherrer formula.

$$D = 0.94 \lambda / \beta \cos \theta \rightarrow (1)$$

Where, D is the average crystallite domain size perpendicular to the reflecting planes, λ is the X-ray wavelength, β is the full width at half maximum (FWHM), and θ is the diffraction angle. To eliminate additional instrumental broadening the FWHM was corrected, using the FWHM from a large grained Si sample.

$$\beta \text{ corrected} = (\text{FWHM2 sample} - \text{FWHM2 si})\ 1/2 \rightarrow (2)$$

This modified formula is valid only when the crystallite size is smaller than 100 nm (Boulch *et al*., 2001).

SEM and AFM analysis of silver nanoparticles: The procedure followed SEM observation of silver nanoparticles below. Sample was prepared by placing a drop of AgNPs on carbon coated copper stuff and subsequently drying air, before transferring it to the microscope operated at an accelerated and voltage of 120KV (JOEL Model JSM-5010 LV with INSA EDS) and followed for Energy Dispersive Spectrophotometer analysis.
The morphology of the product was observed by Nano Surf Easy Scan 2 Atomic Force Microscope (AFM) measurement study the morphology and size of the Ag nanoparticles.

Photocatalytic degradation: The photocatalytic degradation of methyl orange was evaluated by biosynthesized Ag nanoparticles (Rashed and El-Amin 2007). All the experiments were performed outdoor with sun as the main source of light (Wang *et al*., 2000). Prior to the experiment, a suspension was prepared by adding 20 mg of Ag nanoparticles to 50 ml of methyl orange solution (Fisher Scientific). Later, the mixture was allowed to stir constantly for about 30 min in darkness to ensure constant equilibrium of Ag nanoparticles in the organic solution. During the reaction, the mixture was kept under sunlight within a Pyrex glass beaker and stirred constantly. The mean temperature was found to be 29˚C with 10 h mean shine duration. The absorption spectrum of the suspension mixture was measured periodically using a UV–visible spectrophotometer (Shimadzu, UV-2450, Japan) after centrifugation to ensure the degradation of methyl orange solution.

RESULTS AND DISCUSSION

It is well known that silver nanoparticles exhibit reddish brown colour in aqueous solution due to excitation of surface plasmon vibrations in silver nanoparticles (Shankar *et al*., 2004). As the extract was mixed in the aqueous solution of the silver ion complex, it started to change the colour from watery to yellowish brown due to reduction of silver ion which indicated formation of silver nanoparticles (Fig. 1). It is generally recognized that UV–Vis spectroscopy could be used to examine size and shape controlled nanoparticles in aqueous suspensions (Wiley *et al*., 2006). Fig. 2 shows the UV-Vis spectra recorded from the reaction medium after 4 hours.

FT-IR predicts the molecular configuration of different functional group present in the seaweed extract. Considerable absorption peaks by *S. wightii* (Fig. 3) were found at 3279.86 cm^{-1} indicates the presence of N-H stretch (primary, secondary amines), 2953.00 cm^{-1},2922.19 cm^{-1} and 2851.90 cm^{-1} indicates presence of C-H stretch (alkanes), 1723.15 cm^{-1} C=O stretch indicates presence of –C=C- stretch (alkanes), 1528.24 cm^{-1} indicates the presence of N-O asymmetric stretch (nitro compounds), 1450.45 cm-1 indicates the presence of C-C stretch(in-ring) (aromatics), 1379.45 cm^{-1} indicates the presence of C-H

Scissoring bending(alkanes), 1284.76 cm^{-1} and 1260.03 cm^{-1} indicates the presence of C-N stretch (aromatic amines), 1228.85 cm^{-1} and 1043.46 cm^{-1} indicates the presence of C-N stretch (aliphatic amines) and 976.95 cm^{-1} (alkenes). Several species of *Gracilaria* have been reported to contain abundant of amino acids, fatty acids, vitamins, minerals, phenolic compounds and carbohydrates (Yang *et al*., 2012). Of which, phenolic compounds especially polyphenols and tannin have reported to have antimicrobial, anti-carcinogenic and anti-oxidant properties (Arunkumar *et al*., 2010). Satyavani *et al*., 2011 have reported that silver ions may possibly bind to phenolic compounds with one or more aromatic ring resulting in the formation of Ag nanoparticles.

The pattern has three main diffraction features corresponding to (1 1 1), (2 0 0) and (2 2 0) planes and all the three peaks can be indexed to standard cubic phase of silver (JCPDS card No 04-0783). No reflection peaks corresponding to nitrate ions and other impurities were noted in this pattern, indicating the high purity of the final product. Moreover, the obtained reflections are sharp and high in intensity which reveals that the synthesized nanoparticles are well crystalline. In addition, the lattice constant of the synthesized cubic phase of silver is found to be 'a = 4.083 A ° '. This value is consistent with the JCPDS value (a = 4.086 A °). The size of the nanocrystals was determined from the Debye–Scherrer formula D = 0.9k/bcosh, where D is the crystallite size, k is the wavelength of the incident X-ray (1.5406 A °), h is the Bragg's angle and b is the full width at half maximum (FWHM). From the X-ray line broadening the crystallite size of the synthesized products is estimated around 20 nm (r = ±10 %) (Fig.4).

The SEM image (Figure 5a and b) showing the high density Ag-NPs synthesized by the *S. wightii* further confirmed the development of silver nanostructures. The SEM micrographs of nanoparticle obtained in the filtrate showed that Ag-NPs are spherical shaped, well distributed without aggregation in solution. EDS analysis was confirmed the chemical composition of AgNPs. The study significant observed from the atom of Ag.

The surface morphology and size of the Ag nanoparticles harvested after 120 h of incubation were studied by AFM. The two- and three-dimensional images of the nanoparticles were shown in Fig. 6 a and b. From the 2D view, well-separated spherical particles are seen. The sizes of the particles are in the range of 1–40 nm. However, most of the particles are in the range of 10 nm. The 3D view revealed that the growth direction of all the particles was almost same confirming the single crystalline nature of the cubic phase of Ag nanoparticles.

Williams 2008 reported nanoparticles are clusters of atoms in the size range of 1–100 nm. Shanmugam *et al*., 2013 stated that the morphology and size of the synthesized particles were studied with atomic force microscope. Photocatalytic degradation of methyl orange dye was investigated using biometrically synthesized silver nanocatalysts by solar irradiation technique at different time intervals as shown in Fig. 7. The characteristic absorption peak of methyl orange solution was found to be 420 nm. Degradation of methyl orange was visualized by decrease in peak intensity within 10 h of incubation time. Kumar *et al*., (2013) suggested Silver nanoparticles synthesized by facile method from *U. lactuca* can able to degrade dyes in the presence of visible light and paves way for environmental bioremediation. The adsorption of Ag nanoparticles on to the methyl orange solution was initially low and further increased with constant increase in time. Altogether, the photocatalytic properties of Ag nanoparticles in visible light may well be due to excitation of SPR, which is nothing but oscillation of charge density that can propagate at the interface between metal and dielectric medium (Garcia 2011).

CONCLUSIONS

In conclusion, it has been predicted that the extract of marine seaweed *Sargassum wightii* is capable of producing Ag nanoparticles extracellularly and these nanoparticles are quite stable in solution due to capping likely by the proteins present in the extract. This is an efficient, eco-friendly and simple process. The presence of functional bioactive compounds in seaweed extract is responsible for the formation of Ag nanoparticles as revealed by FTIR. The average size of spherical-shaped Ag nanoparticles ranges between 05 and 40 nm. The XRD and SEM analysis showed the particle size between 25-50 nm as well the cubic structure of the nanoparticles. This green chemistry approach toward the synthesis of silver nanoparticles has many advantages such as, ease with which the process can be scaled up, economic viability, etc.

Fig. 1 C. Silver nitrate ($AgNO_3$) solution and others colour changes during the reduction of $AgNO_3$ into AgNPs by the extract of *S. wightii* after 20 min of incubation

Fig. 2 UV–visible absorption spectrum of silver nanoparticles after 30 min of incubation

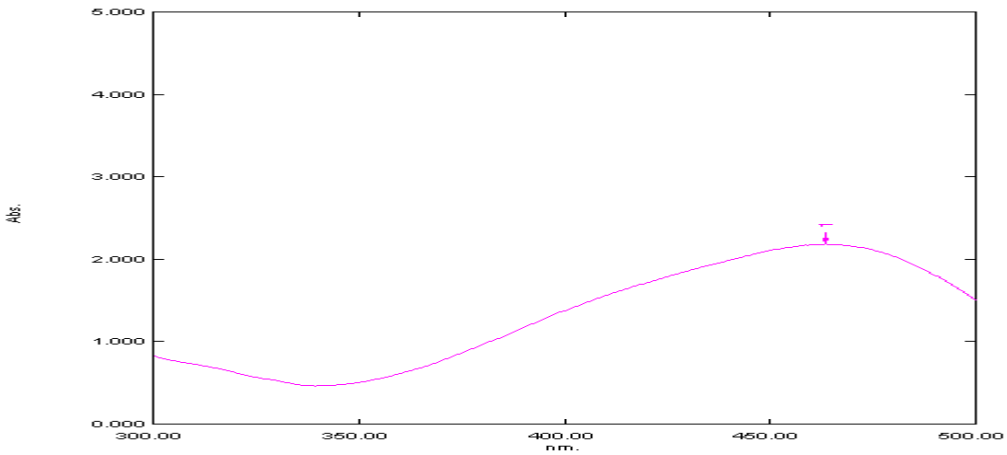

Fig. 3 FT-IR spectrum of $AgNO_3$ into AgNPs by the extract of *S.wightii*.

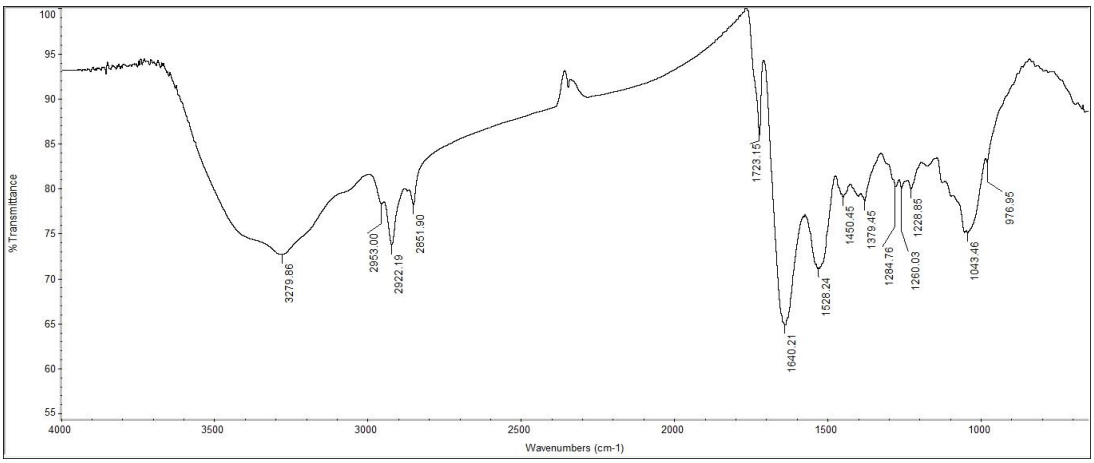

Fig. 4 XRD patterns of silver nanoparticles synthesized after 120 h of incubation

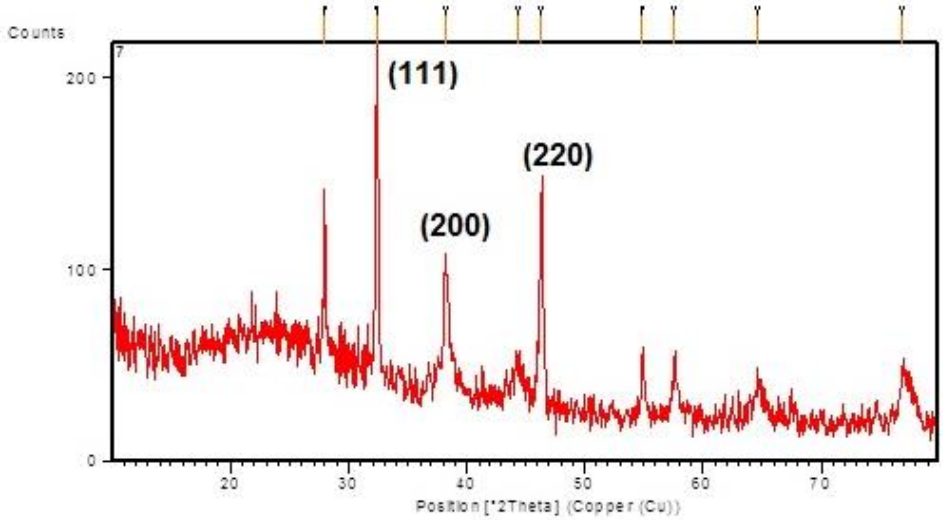

Fig. 5 (A) SEM micrograph of Silver nanoparticles synthesized from the extracts of *S.wightii* and (B) Energy dispersive spectrometer analysis

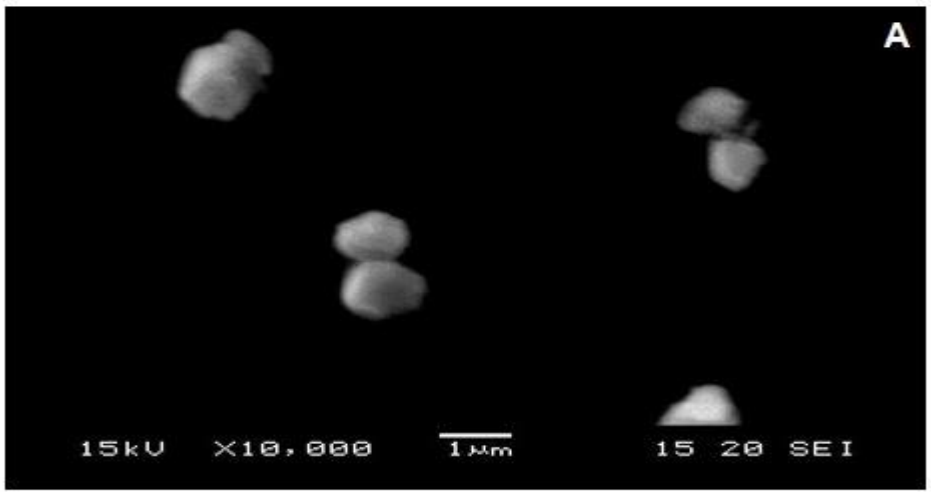

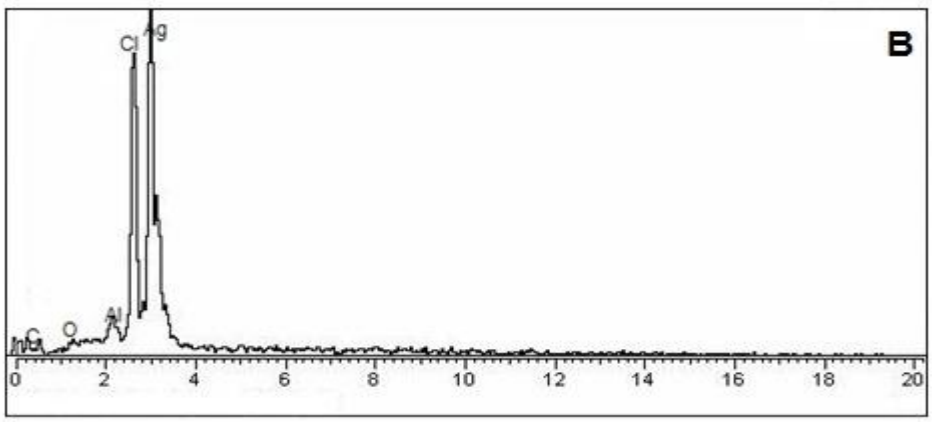

Fig. 6 (A) AFM images of synthesized silver nanoparticles using extract of *S. wightii* and (B) corresponding 3D view

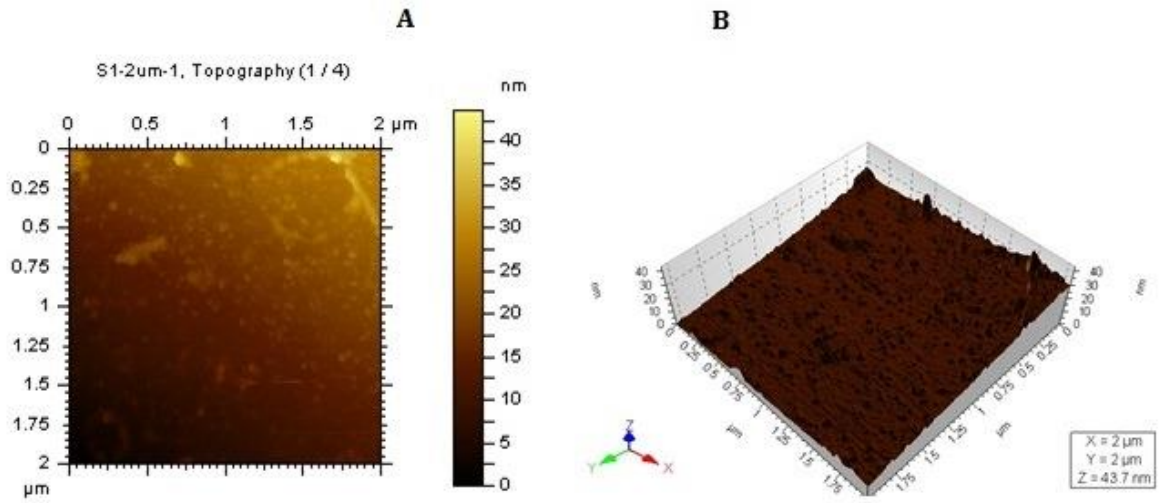

Fig. 7. Photocatalytic degradation of methyl orange using silver nanoparticles synthesized from *S. wightii*.

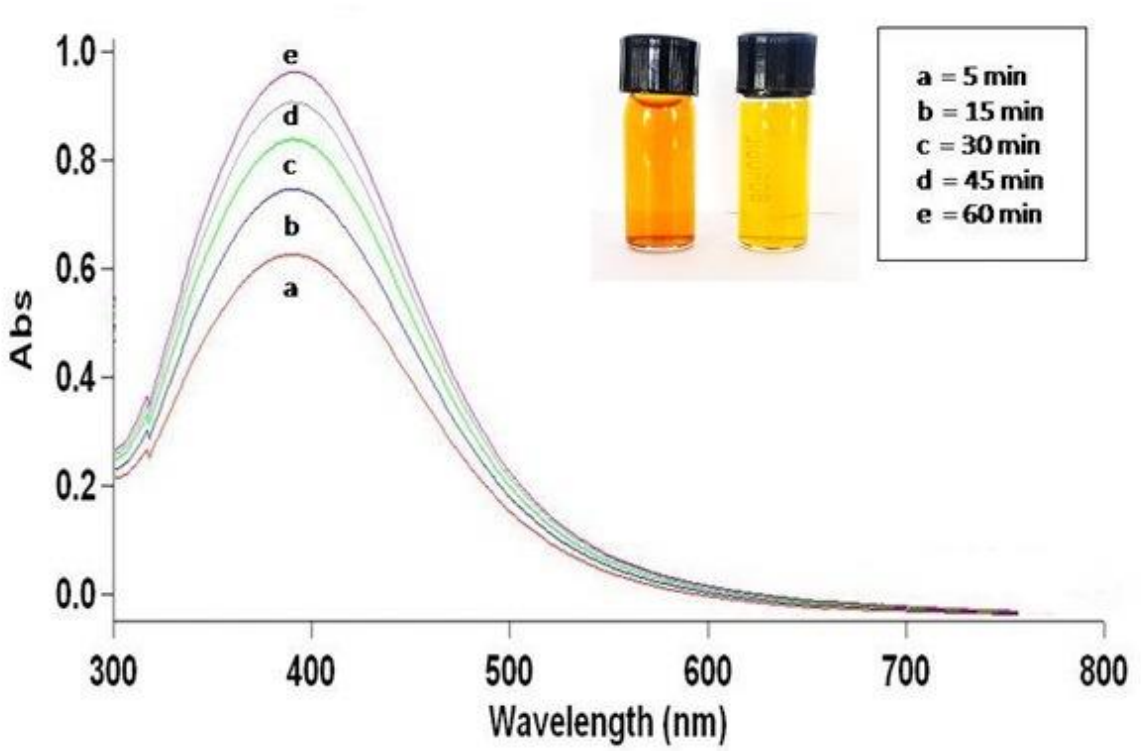

REFERENCES

1. Jahn W., J. Struc. Biol. 1999; 127:106.
2. Naiwa HS. Ed. Hand Book of Nanostructural Materials and Nanotechnology. Academic Press New York. 2000; 1-5.
3. Murphy CJ. Sustainability as a design criterion in nanoparticle synthesis and applications. J. Mat. Chem., 2008; 18: 2173–2176.
4. Kwakye-Awuah, B., Williams, C., Kenward, MA. and Radecka, I. Antimicrobial action and efficiency of silver-loaded zeolite X. J. Appli. Microb. 2008; 104:1516–1524.
5. Silver, S., Phung, LT. and Silver, G. Silver as biocides in burn and wound dressings and bacterial resistance to silver compounds. J. Indus. Microb. and Biotech. 2006; 33: 627– 34.
6. Rashed MN, El-Amin AA. Int. J. of Phy. Sci. 2007; 2:73.
7. Shankar SS, Rai A, Ankamwar B, Singh A, Ahmad A, Sastry M. Nat. Material. 2004; 3: 482.
8. Shanmugam N, Rajkamal P, Cholan S, Kannadasan N, Sathishkumar K, Viruthagiri G, Sundaramanickam A. Biosynthesis of silver nanoparticles from the marine seaweed *Sargassum wightii* and their antibacterial activity against some human pathogens. Appl. Nanosci. DOI 10.1007/s13204-013-0271-4. 2013.
9. Wang G, Liao C, Wu F. Chemosphere. 2000; 42:379.
10. Williams D. The relationship between biomaterials and nanotechnology. Biomater. 2008; 29:1737.
11. Wiley BJ, Im SH, McLellan J, Siekkinen A. Xia Y. J. of Phy. and Chem.:B. 2006; 110:15666.
12. Ahmad A, Mukherjee P, Senapati S, Mandal D, Khan MI, Kumar R, Sastry M. Extracellular biosynthesis of silver nanoparticles using the fungus *Fusarium oxysporium*. Colloids and Surface B: Interface. 2003; 28:313–318.
13. Arunkumar K, Sivakumar SR, Rengasamy R. Review on Bioactive potential in seaweeds (Marine Macroalgae): a special emphasis on biodiversity of seaweeds against plant pathogens. Asian J. Plant Sci. 2010; 9:227–240.
14. Kumar P, Senthamilselvi S, Lakshmipraba A, Premkumar K, Muthukumaran R, Visvanathan P, Ganeshkumar RS, Govindaraju M. Efficacy of biosynthesized silver nanoparticles using *Acanthophora spicifera* to encumber biofilm formation. Dig. J. of Nanomat. Biosci. 2012a; 7:511–522.
15. Mohanpuria P, Rana NK, Yadav SK. Biosynthesis of nanoparticles: technological concepts and future applications. J. Nanopart. Res. 2008; 10:507–517.
16. Ramanathan R, O'Mullane AP, Parikh RY, Smooker PM, Bhargava SK, Bansal V. Bacterial kinetics-controlled shape-directed biosynthesis of silver nanoplates using *Morganella psychrotolerans*. Langmuir. 2011; 27(2):714–719.
17. Satyavani K, Gurudeeban S, Ramanathan T, Balasubramanian T. Biomedical potential of silver nanoparticles synthesized from calli cells of *Citrullus colocynthis* (L.). J. Nanobiot. 2011; 9:43–50.
18. Shankar SS, Ahmad A, Sastry M. Geranium leaf assisted biosynthesis of silver nanoparticles. Biotech. Prog. 2003; 19: 1627–1631.
19. Yang JI, Yeh CC, Lee JC, Yi SC, Huang HW, Tseng CN, Chang HW. Aqueous extracts of the edible *Gracilaria tenuistipitata* are protective against H_2O_2-induced DNA damage, growth inhibition, and cell cycle arrest. Molecules. 2012; 17:7241–7254.
20. Kumar P, Govindaraju M, Senthamilselvi S, Premkumar K. Photocatalytic degradation of methyl orange dye using silver (Ag) nanoparticles synthesized from *Ulva lactuca*. Coll. and Surf. B: Biointer. 2013; 103: 658– 661.
21. Garcia, MA. Surface plasmons in metallic nanoparticles: fundamentals and applications. J. Phy. D: Appl. Phy. 2011; 44: 28, 283001.